New Investigations on the Method of Characteristics for the Evaluation of Line Transients

Thomas Kauffmann, Ilhan Kocar, Jean Mahseredjian

***Abstract*—The Method of Characteristics (MoC) transforms line equations into ordinary differential equations and the transient solution is performed numerically through discretization in time and space. Recently, it has been proposed in the literature to drop discretization in space for uniform lines. This has the potential to render the MoC faster than the traveling wave based models. This paper investigates in detail the possibility of removing spatial discretization and contributes step by step clarifications on the application of MoC for the evaluation of line transients. It has been demonstrated that although removing spatial discretization is possible by introducing certain change of variables and approximations, the resulting model has limited numerical precisions. This is principally due to the approximation error introduced by the linearization of differential equations, necessary to obtain a relationship between line ends. The paper discusses other sources of numerical imprecision and shows that numerical precision improves as the line is subdivided.**

***Index Terms*— Method of characteristics, transient analysis, transmission lines, frequency and time domain analysis**

I. Introduction

The most common transient solution method of lines is based on traveling wave equations and obtained by transforming the frequency domain equations into time domain. In the frequency domain, lines and cables are characterized with two frequency dependent coefficients: the propagation function $\mathbf{H}$ and the characteristic admittance $\mathbf{Y_c}$. The basic idea of the frequency dependent models in Electromagnetic Transient Type (EMT-type) programs is to use rational function approximations for these coefficients obtained by using fitting techniques to allow efficient computation of convolution integrals through recursive schemes. The Universal Line Model (ULM) is considered here as the state-of-the art model in terms of application flexibility and precision [1]. The recent research in this field is on the passivity enforcement of models [2], improvement of numerical stability [3]-[5] and real time implementation [6].

Another class of transient solution techniques is based on the application of Method of Characteristic (MoC). This technique transforms the partial differential equations (PDEs) into sets of Ordinary Differential Equations (ODEs) directly in time domain by using characteristic curves. It was successfully applied to study corona on transmission lines with constant parameters [7], [8]. Recent research efforts not only focus on the frequency dependence of parameters but also deal with non-linear [9], external field-excited [10] and non-uniform transmission lines [11]. The MoC requires spatial discretization in addition to discretization in time. Therefore, the solution is inefficient for uniform lines compared to traveling wave models such as ULM. On the other hand, it has been recently proposed to remove spatial discretization for uniform lines by using the relationship on the propagation speed of modal waves along characteristic curves [12]-[13]. This approach seems promising since the removal of spatial discretization has the potential to render the technique very efficient due to the following key advantages:

- As opposed to two convolutions for each end in traveling wave models only one convolution is required
- Traveling wave models require the fitting of $\mathbf{H}$ and $\mathbf{Y_c}$. In the MoC, however, the series impedance elements are needed to be fit, which are smoother.

This paper first presents a fitting procedure for series impedance elements and then contributes important theoretical clarifications on the application of MoC with and without spatial discretization, identifies the sources of numerical errors, and discusses variations for improvement. It is shown that the fundamental source of numerical problems is the approximation error arising from the linearization of differential equations relating line terminal variables. A large integration step dictated by the modal delays is required when it is desired to avoid spatial discretization. The paper concludes that the line should be subdivided to improve numerical precision and maintain stability. The subdivision of line however supresses the expected numerical advantages over traveling wave methods for uniform lines.

II. Frequency Dependent Model in Time Domain

This section shows the development of line equations in time domain while considering the frequency dependence. To emphasize the frequency dependence of electrical parameters, it is helpful first to write the distributed line equations in frequency domain. For a transmission line with n conductors:

$$-\frac{d\,\mathbf{V}(x,s)}{dx}=\mathbf{Z}(s)\mathbf{I}(x,s),\ -\frac{d\,\mathbf{I}(x,s)}{dx}=\mathbf{Y}(s)\mathbf{V}(x,s) \quad (1)$$

In (1) s is the Laplace operator, x is the spatial variable along which the waves propagate, $\mathbf{V}$ and $\mathbf{I}$ are voltage and current vectors, $\mathbf{Z}$ is the series impedance matrix and $\mathbf{Y}$ is the shunt admittance matrix, both per unit length. For a line of n

T. Kauffmann is with the Department of Electrical Engineering, Polytechnique Montreal, QC, Canada (email: Thomas.kauffmann@polymtl.ca).
I. Kocar is with the Department of Electrical Engineering, Polytechnique Montreal, QC, Canada (email of corresponding author: ilhan.kocar@polymtl.ca)
J. Mahseredjian is with the Department of Electrical Engineering, Polytechnique Montreal, QC, Canada (email: jean.mahseredjian@polymtl.ca)

Paper submitted to the International Conference on Power Systems Transients (IPST 2017) in Seoul, South Korea June 26-29, 2017.

conductors, the size of the matrices is n-by-n and the size of the vectors is n-by-1.

The transformation of (1) into time domain results in convolution integrals which need to be computed over discrete time steps when the model is hosted in an EMT-type program. The approximation of frequency dependent coefficients with analytical functions leads to efficient computation of convolution integrals. The following rational form can be used for the fitting of $\mathbf{Z}$

$$\mathbf{Z}(\mathrm{s}) \cong \mathbf{R}_{DC} + s\left(\mathbf{D} + \sum_{i=1}^{N} \frac{\mathbf{K}_i}{s - p_i}\right) \tag{2}$$

if s is realised as complex frequency, then $\mathbf{R}_{DC}$ represents the DC resistance matrix, $\mathbf{D}$ corresponds to a constant matrix of inductance, $\mathbf{K}_i$ is the matrix of residues associated with the pole p_i and N is the number of poles used for fitting. The rational function accounts for the frequency dependence of resistance and inductance.

A similar form for the shunt admittance matrix is used but only the equivalent of $\mathbf{D}$ is kept since the conductance and the frequency variation of parameters can usually be neglected:

$$\mathbf{Y}(\mathrm{s}) = s\mathbf{C} \tag{3}$$

In (3), $\mathbf{C}$ is the shunt capacitance matrix and it is constant.

A. Fitting Procedure

Since the fitting quality plays an important role in simulation precision, an efficient fitting procedure is contributed here. First, (2) is rearranged as follows:

$$\frac{1}{s}\left(\mathbf{Z}(\mathrm{s}) - \mathbf{R}_{DC}\right) \cong \mathbf{D} + \sum_{i=1}^{N} \frac{\mathbf{K}_i}{s - p_i} \tag{4}$$

The matrix $\mathbf{R}_{DC}$ is obtained by using a very low frequency sample, then the diagonal elements of the left hand side of (4) are summed and the vector fitting (VF) method [14] is applied in order to identify the common poles for each entry in the matrix. Following the identification of poles, $\mathbf{K}_i$ and $\mathbf{D}$ are computed using an overdetermined linear system of equations. Note that a wideband frequency range (typically from a few millihertz to a few MHz) and several frequency samples (typically 100-200) are used to construct the overdetermined system of equations for both stages of fitting.

One remark in the solution of (4) is related to $\mathbf{D}$. It should correspond to a constant line inductance at high frequencies and letting it be an unknown variable has one sole purpose of relaxing the fitting process and minimizing the order of fitting. However, the fitting result should be checked carefully if the product $\mathbf{DC}$ produces realistic modal velocities otherwise it is advisable to fix $\mathbf{D}$ by using a high frequency sample and move it to the left hand side of (4).

B. Back to Time Domain

Once the series impedance and shunt admittance matrices are realized with (2) and (3), they are inserted into the line equations in (1). Then, the transformation of equations into time domain results in:

$$\frac{\partial \mathbf{i}(x,t)}{\partial x} + \mathbf{C}\frac{\partial \mathbf{v}(x,t)}{\partial t} = \mathbf{0} \tag{5}$$

$$\begin{aligned} &\frac{\partial \mathbf{v}(x,t)}{\partial x} + \mathbf{D}\frac{\partial \mathbf{i}(x,t)}{\partial t} + \mathbf{R}_{DC}\mathbf{i}(x,\mathrm{t}) \\ &+ \frac{\partial}{\partial t}\int_0^t \mathbf{h}(t-\tau)\mathbf{i}(x,\tau)\,d\tau = \mathbf{0} \end{aligned} \tag{6}$$

where

$$\mathbf{h}(t) = \sum_{i=1}^{N} e^{p_i t}\mathbf{K}_i. \tag{7}$$

In (6), the derivative can be moved inside the integral yielding:

$$\frac{\partial \mathbf{v}(x,t)}{\partial x} + \mathbf{D}\frac{\partial \mathbf{i}(x,t)}{\partial t} + \mathbf{R}_h\mathbf{i}(x,\mathrm{t}) + \boldsymbol{\Psi}(x,t) = \mathbf{0} \tag{8}$$

with

$$\mathbf{R}_h = \mathbf{R}_{DC} + \sum_{i=1}^{N}\mathbf{K}_i \tag{9}$$

$$\boldsymbol{\Psi}(x,t) = \sum_{i=1}^{N} p_i\mathbf{K}_i\left[e^{p_i t} * \mathbf{i}(x,\mathrm{t})\right] \tag{10}$$

where the symbol * denotes convolution.

The equations (5) and (8) form a system of two PDEs governing voltage and current waves along the line and they take into account the frequency dependence of series impedance.

III. Method of Characteristics

This section describes the application of the method of characteristics which seeks to transform the PDEs into ODEs. The voltage and current variables in the system of PDEs above are in phase domain and they need to be first transformed such that each variable gets associated with a single modal velocity. To this end the following transformation matrices are introduced:

$$\mathbf{T}_V^{-1}\mathbf{DCT}_V = \boldsymbol{\Lambda} \tag{11}$$

$$\mathbf{T}_I^{-1}\mathbf{CDT}_I = \boldsymbol{\Lambda} \tag{12}$$

where $\boldsymbol{\Lambda}$ is a diagonal matrix. Note that $\mathbf{C}$ and $\mathbf{D}$ are constant matrices so there is no need to introduce frequency dependent transformation matrices. Note that $\boldsymbol{\Lambda}$ is associated with modal velocities:

$$\boldsymbol{\Gamma} = \sqrt{\boldsymbol{\Lambda}^{-1}} = diag\left(\gamma_1,\ldots,\gamma_n\right) \tag{13}$$

The modal velocities (γ_i) are always positive and are related to the derivative dx/dt. According to the direction of the wave, the derivative dx/dt is positive (from sending end to receiving end) or negative (from receiving end to sending end). Therefore, the characteristic curves in the *x, t* plane are given by

$$\begin{aligned} \boldsymbol{\Gamma} &= diag\left(\frac{dx_1}{dt},\ldots,\frac{dx_n}{dt}\right) \\ \boldsymbol{\Gamma} &= -diag\left(\frac{dx_1}{dt},\ldots,\frac{dx_n}{dt}\right) \end{aligned} \tag{14}$$

The transformation matrices are then used to convert the voltages and currents in modal domain:

$$\mathbf{v}(x,t) = \mathbf{T}_V\,\mathbf{v}_m(x,t),\ \ \mathbf{i}(x,t) = \mathbf{T}_I\,\mathbf{i}_m(x,t) \tag{15}$$

The system of equations in modal domain is given by:

$$\frac{\partial \mathbf{i}_m(x,t)}{\partial x} + \mathbf{C}_m \frac{\partial \mathbf{v}_m(x,t)}{\partial t} = \mathbf{0} \tag{16}$$

$$\frac{\partial \mathbf{v}_m(x,t)}{\partial x} + \mathbf{D}_m \frac{\partial \mathbf{i}_m(x,t)}{\partial t} + \mathbf{R}_m \mathbf{i}_m(x,t) + \mathbf{\Psi}_m(x,t) = \mathbf{0} \tag{17}$$

with

$$\mathbf{D}_m = \mathbf{T}_V^{-1}\mathbf{D}\mathbf{T}_I \qquad \mathbf{C}_m = \mathbf{T}_I^{-1}\mathbf{C}\mathbf{T}_V \qquad \mathbf{R}_m = \mathbf{T}_V^{-1}\mathbf{R}_h\mathbf{T}_I \tag{18}$$

$$\mathbf{\Psi}_m(x,t) = \mathbf{T}_V^{-1}\sum_{i=1}^{N} p_i \mathbf{K}_i \left[e^{p_i t} * \mathbf{T}_I \mathbf{i}_m(x,t) \right] \tag{19}$$

Note that $\mathbf{D}_m$ and $\mathbf{C}_m$ are diagonal. $\mathbf{R}_m$ like $\mathbf{R}_h$ is a full matrix whereas $\mathbf{\Psi}_m$ is the vector containing the convolution.

It is also possible to write $\mathbf{\Lambda}$ in terms of modal parameters.

$$\mathbf{\Lambda} = \mathbf{C}_\mathrm{m}\mathbf{D}_\mathrm{m} = \mathbf{D}_\mathrm{m}\mathbf{C}_\mathrm{m} \tag{20}$$

If the wave impedance matrix is defined as:

$$\mathbf{Z}_w = \sqrt{\mathbf{D}_m \mathbf{C}_m^{-1}} \tag{21}$$

the system of equations becomes:

$$\mathbf{\Gamma}\frac{\partial \mathbf{v}_m}{\partial x} + \mathbf{Z}_w \frac{\partial \mathbf{i}_m}{\partial t} + \mathbf{\Gamma}\mathbf{R}_m\mathbf{i}_m + \mathbf{\Gamma}\mathbf{\Psi}_m = \mathbf{0} \tag{22}$$

$$\mathbf{\Gamma}\mathbf{Z}_w \frac{\partial \mathbf{i}_m}{\partial x} + \frac{\partial \mathbf{v}_m}{\partial t} = \mathbf{0} \tag{23}$$

The key point of the MoC is to transform this system of PDEs into ODEs. This can be done by introducing the total derivative expression for voltage and current

$$\begin{aligned} d\mathbf{v}_m &= \frac{\partial \mathbf{v}_m}{\partial x}dx + \frac{\partial \mathbf{v}_m}{\partial t}dt \\ d\mathbf{i}_m &= \frac{\partial \mathbf{i}_m}{\partial x}dx + \frac{\partial \mathbf{i}_m}{\partial t}dt \end{aligned} \tag{24}$$

and by replacing the dx/dt terms with $\mathbf{\Gamma}$.

The resulting equations are summed and subtracted to remove the partial differentiation, and the following set of ODEs is obtained:

$$\frac{d\mathbf{v}_m}{dt} + \mathbf{Z}_w \frac{d\mathbf{i}_m}{dt} + \mathbf{\Gamma}\mathbf{R}_m\mathbf{i}_m + \mathbf{\Gamma}\mathbf{\Psi}_m = \mathbf{0} \tag{25}$$

$$\frac{d\mathbf{v}_m}{dt} - \mathbf{Z}_w \frac{d\mathbf{i}_m}{dt} - \mathbf{\Gamma}\mathbf{R}_m\mathbf{i}_m - \mathbf{\Gamma}\mathbf{\Psi}_m = \mathbf{0} \tag{26}$$

The first one corresponds to the wave travelling from the sending end, and the second one from the receiving end. Note that the convolution term still contains the variable *x*. The line transients can be computed by numerically solving (25) and (26).

IV. Resolution and Implementation

It is necessary to define spatial boundaries in order to numerically solve the ODEs of (25) and (26). In [13] it is proposed to take the sending and receiving ends as the boundaries of the system and apply trapezoidal method to linearize the ODEs and avoid spatial discretization. If the delay associated with the fastest mode is τ the following equations are obtained by applying trapezoidal method to the ODEs (only one equation is shown since the other one can be obtained by changing signs)

$$\frac{\mathbf{v}_{R,m}^{t} - \mathbf{v}_{S,m}^{t-\tau}}{\tau} + \mathbf{Z}_w \frac{\mathbf{i}_{R,m}^{t} - \mathbf{i}_{S,m}^{t-\tau}}{\tau} + \mathbf{\Gamma}\mathbf{R}_m \left(\frac{\mathbf{i}_{R,m}^{t} + \mathbf{i}_{S,m}^{t-\tau}}{2} \right) + \mathbf{\Gamma}\left(\frac{\mathbf{\Psi}_{R,m}^{t} + \mathbf{\Psi}_{S,m}^{t-\tau}}{2} \right) = \mathbf{0} \tag{27}$$

by rearranging the terms

$$\mathbf{v}_{R,m}^{t} - \mathbf{v}_{S,m}^{t-\tau} + \mathbf{Z}_w\left(\mathbf{i}_{R,m}^{t} - \mathbf{i}_{S,m}^{t-\tau}\right) + \frac{\boldsymbol{l}}{2}\mathbf{R}_m\left(\mathbf{i}_{R,m}^{t} + \mathbf{i}_{S,m}^{t-\tau}\right) + \frac{\boldsymbol{l}}{2}\left(\mathbf{\Psi}_{R,m}^{t} + \mathbf{\Psi}_{S,m}^{t-\tau}\right) = \mathbf{0} \tag{28}$$

where

$$\boldsymbol{l} = \tau\mathbf{\Gamma} \tag{29}$$

$\boldsymbol{l}$ is a diagonal matrix in which each element corresponds to the distance travelled by the modes during τ time.

A. Discussion of Numerical Errors

It should be noted that the trapezoidal approximation is performed over a large time step (τ) in (28) and this is the main source of numerical imprecision that increases with the line length. This is overlooked in [13]. A practical solution to reduce the error is to increase the resolution, i.e., to subdivide the line into short sections and take the receiving end of one section as the sending end of the next section. Although this will increase the arithmetic operations it is necessary to set better precisions as will be demonstrated through a case study.

Using trapezoidal approximation over short line segments becomes eventually comparable to the application of spatial discretization and central differences [10] in terms of numerical burden.

Note that, as shown in Fig. 1, once the fastest modal wave reaches the other end of the line after τ time, the others will be lagging although they will be very close to the end (a few percent in distance for most lines). In (27) all modal waves are considered to arrive in τ time. To minimize the error due to this assumption, spatial interpolation can be performed for slower modal waves. In this study, we also used a vector of time delays in (27) and totally avoided spatial interpolation:

$$\boldsymbol{\tau}^{-1}\left(\mathbf{v}_{R,m}^{t} - \mathbf{v}_{S,m}^{t-\tau}\right) + \mathbf{Z}_w\boldsymbol{\tau}^{-1}\left(\mathbf{i}_{R,m}^{t} - \mathbf{i}_{S,m}^{t-\tau}\right) + \mathbf{\Gamma}\mathbf{R}_m\left(\frac{\mathbf{i}_{R,m}^{t} + \mathbf{i}_{S,m}^{t-\tau}}{2}\right) + \mathbf{\Gamma}\left(\frac{\mathbf{\Psi}_{R,m}^{t} + \mathbf{\Psi}_{S,m}^{t-\tau}}{2}\right) = 0 \tag{30}$$

where $\boldsymbol{\tau}$ in bold character is a diagonal matrix containing all propagation delays. The terms at $t-\boldsymbol{\tau}$, such as $\mathbf{v}_{S,m}^{t-\tau}$ consist of different delays.

$$\mathbf{v}_{S,m}^{t-\tau} = \begin{cases} \mathbf{v}_{S,m,1}^{t-\tau 1} \\ \mathbf{v}_{S,m,2}^{t-\tau 2} \\ \vdots \\ \mathbf{v}_{S,m,n}^{t-\tau n} \end{cases} \tag{31}$$

Based on the several cases that we studied, not a significant improvement has been observed by avoiding spatial discretization. Therefore, it is concluded that spatial interpolation is not the main source of numerical imprecision.

The implementation of the method in an EMT-type solver requires another approximation: interpolation in time for the evaluation of historical terms at $t-\tau$. This is done since τ is not necessarily an integer multiple of the time step of the simulation and the variables at $t-\tau$ are simply not available. In practice, the time interpolation is done first to have voltages and currents at the ends of the transmission system then the space interpolation is done for the slower modes.

About the numerical stability of (27) it can be seen that the discretization satisfies the Courant-Friedrichs-Lewi condition given by

$$\Delta x = \max(\gamma_1,\ldots,\gamma_n)\Delta t \tag{32}$$

since Δx corresponds to the length of the line while Δt corresponds to the delay of the fastest mode τ.

B. Recursive Convolution

The convolution product is hidden in the variable $\boldsymbol{\Psi}$. This product is solved in a recursive way as explained next.

The procedure starts with the expression in frequency domain:

$$\boldsymbol{\Psi}_m(x,s) = \mathbf{T}_V^{-1}\sum_{i=1}^{N}\left(\frac{p_i\,\mathbf{K}_i}{s-p_i}\right)\mathbf{T}_I\mathbf{I}_m(x,s) \tag{33}$$

We define

$$\boldsymbol{\Psi}_m(x,s) = \sum_{i=1}^{N}\boldsymbol{\psi}_i(x,s) \tag{34}$$

where

$$\boldsymbol{\psi}_i(x,s) = \frac{p_i}{s-p_i}\mathbf{T}_V^{-1}\mathbf{K}_i\mathbf{T}_I\mathbf{I}_m(x,s) \tag{35}$$

The equation is rearranged and then transformed into time domain:

$$(s-p_i)\boldsymbol{\psi}_i(x,s) = p_i\,\mathbf{T}_V^{-1}\mathbf{K}_i\mathbf{T}_I\mathbf{I}_m(x,s) \tag{36}$$

$$\frac{d}{dt}\boldsymbol{\psi}_i(x,t) - p_i\boldsymbol{\psi}_i(x,t) = p_i\,\mathbf{T}_V^{-1}\mathbf{K}_i\mathbf{T}_I\mathbf{i}_m(x,t) \tag{37}$$

The differential equation can be numerically solved using the algorithms commonly employed in EMT-type programs such as Trapezoidal or Backward Euler. The Backward Euler solution is given below:

$$\frac{\boldsymbol{\psi}_i^t(x)-\boldsymbol{\psi}_i^{t-\Delta t}(x)}{\Delta t} - p_i\boldsymbol{\psi}_i^t(x) = p_i\,\mathbf{T}_V^{-1}\mathbf{K}_i\mathbf{T}_I\mathbf{i}_m^t(x) \tag{38}$$

with Δt being the time step of EMTP.
Rearranging (38) gives

$$\boldsymbol{\psi}_i^t(x) = \frac{\boldsymbol{\psi}_i^{t-\Delta t}(x)}{1-\Delta t\,p_i} + \frac{\Delta t\,p_i}{1-\Delta t\,p_i}\mathbf{T}_V^{-1}\mathbf{K}_i\mathbf{T}_I\mathbf{i}_m^t(x) \tag{39}$$

Therefore

$$\boldsymbol{\Psi}_m(x,t) = \sum_{i=1}^{N}\frac{\boldsymbol{\psi}_i^{t-\Delta t}(x)}{1-\Delta t\,p_i} + \mathbf{T}_V^{-1}\sum_{i=1}^{N}\left(\frac{\Delta t\,p_i\,\mathbf{K}_i}{1-\Delta t\,p_i}\right)\mathbf{T}_I\mathbf{i}_m^t(x) \tag{40}$$

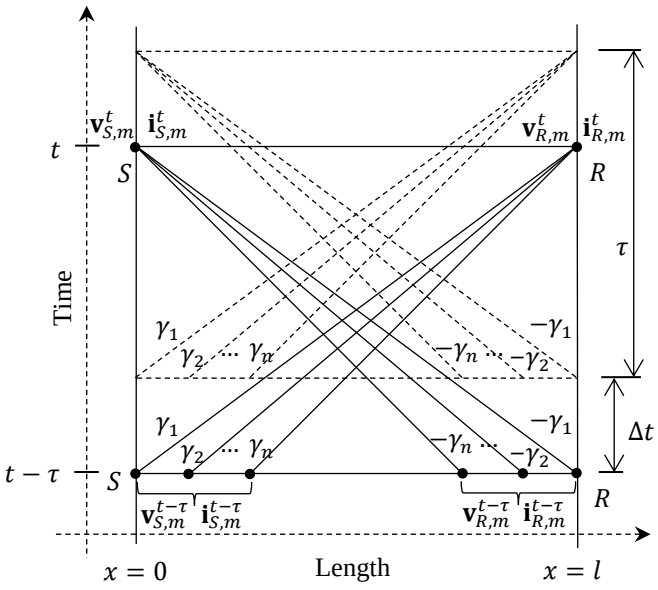

Fig. 1 Modal voltages and currents

It is essential to notice that $\boldsymbol{\Psi}^t$ contains variables of time t which are being updated. Consequently, $\boldsymbol{\Psi}^t$ should be separated in two parts. To this end, the sum on the left part of (40) is abbreviated with $\boldsymbol{\varphi}^t$ and the right one is included in $\mathbf{Z}_K$ as defined in (44).

The equation (28) is rearranged in terms of time and location using the new variables:

$$\mathbf{v}_{R,m}^t - \mathbf{v}_{S,m}^{t-\tau} + \mathbf{Z}_K\mathbf{i}_{R,m}^t - \mathbf{Z}_1\mathbf{i}_{S,m}^{t-\tau} + 0.5\boldsymbol{l}\left(\boldsymbol{\varphi}_{R,m}^t + \boldsymbol{\Psi}_{S,m}^{t-\tau}\right) = \mathbf{0} \tag{41}$$

The same steps are applied to (26) for waves moving from the receiving end to the sending end, the final equation is:

$$\mathbf{v}_{S,m}^t - \mathbf{v}_{R,m}^{t-\tau} - \mathbf{Z}_K\mathbf{i}_{S,m}^t + \mathbf{Z}_1\mathbf{i}_{R,m}^{t-\tau} - 0.5\boldsymbol{l}\left(\boldsymbol{\varphi}_{S,m}^t + \boldsymbol{\Psi}_{R,m}^{t-\tau}\right) = \mathbf{0} \tag{42}$$

with

$$\mathbf{Z}_1 = \mathbf{Z}_w - 0.5\boldsymbol{l}\,\mathbf{R}_m \tag{43}$$

$$\mathbf{Z}_K = \mathbf{Z}_w + 0.5\boldsymbol{l}\,\mathbf{R}_m + 0.5\boldsymbol{l}\Delta t\,\mathbf{T}_V^{-1}\sum_{i=1}^{N}\left(\frac{p_i\,\mathbf{K}_i}{1-\Delta t\,p_i}\right)\mathbf{T}_I \tag{44}$$

$$\boldsymbol{\varphi}_{R,m}^t = \sum_{i=1}^{N}\left(\frac{\boldsymbol{\Psi}_{R,i}^{t-\Delta t}}{1-\Delta t\,p_i}\right) \tag{45}$$

$$\boldsymbol{\varphi}_{S,m}^t = \sum_{i=1}^{N}\left(\frac{\boldsymbol{\Psi}_{S,i}^{t-\Delta t}}{1-\Delta t\,p_i}\right) \tag{46}$$

It is now possible to isolate variables at time t and define historical terms as follows:

$$\mathbf{v}_{R,m}^t + \mathbf{Z}_K\mathbf{i}_{R,m}^t = \mathbf{v}_{H,m}^S \tag{47}$$

$$\mathbf{v}_{S,m}^t - \mathbf{Z}_K\mathbf{i}_{S,m}^t = \mathbf{v}_{H,m}^R \tag{48}$$

where

$$\mathbf{v}_{H,m}^S = \mathbf{v}_{S,m}^{t-\tau} + \mathbf{Z}_1\mathbf{i}_{S,m}^{t-\tau} - 0.5\boldsymbol{l}\left(\boldsymbol{\varphi}_{R,m}^t + \boldsymbol{\Psi}_{S,m}^{t-\tau}\right) \tag{49}$$

$$\mathbf{v}_{H,m}^R = \mathbf{v}_{R,m}^{t-\tau} - \mathbf{Z}_1\mathbf{i}_{R,m}^{t-\tau} + 0.5\boldsymbol{l}\left(\boldsymbol{\varphi}_{S,m}^t + \boldsymbol{\Psi}_{R,m}^{t-\tau}\right) \tag{50}$$

Finally, the system can be transformed back into phase domain:

$$\mathbf{i}_S^t = \mathbf{Y}_{phase}^K \mathbf{v}_S^t + \mathbf{i}_H^R \quad (51)$$

$$\mathbf{i}_R^t = -\mathbf{Y}_{phase}^K \mathbf{v}_R^t - \mathbf{i}_H^S \quad (52)$$

with

$$\mathbf{i}_H^S = -\mathbf{T}_I \mathbf{Z}_K^{-1} \mathbf{v}_{H,m}^S \quad (53)$$

$$\mathbf{i}_H^R = -\mathbf{T}_I \mathbf{Z}_K^{-1} \mathbf{v}_{H,m}^R \quad (54)$$

$$\mathbf{Y}_{phase}^K = \mathbf{T}_I \mathbf{Z}_K^{-1} \mathbf{T}_V^{-1} \quad (55)$$

The equations (51) and (52) provide the Norton equivalent of the line to be used in EMT-type solvers as shown in Fig. 2:

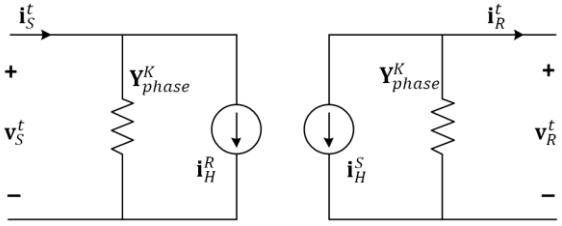

Fig. 2 Norton model of a transmission line

The convolution products and the historical terms need to be updated at each time step.

V. Simulation Examples

A. Multiconductor Case

The Fig. 3 presents a transmission line case. The electrical parameters are obtained using line constants in EMTP-RV [16] and the results are compared to the ULM implementation in that software.

The length of the line is 300km and the ground return resistivity is 100 Ωm . Each phase is a bundle of 2 wires having a diameter of 4.06908 cm and a DC resistance of 0.0324 Ω/km (per wire). The sagging between towers is not considered.

The phases A, B and C are energized at 2, 6 and 12 ms respectively with a balanced AC source. A time step of 10 μs is used. The fitting of $\mathbf{Z}$ can be achieved with 10 poles as shown in Fig. 4.

The Fig. 5 to Fig. 8 present the significant difference between waveforms obtained with EMTP-RV and with the MoC when the line is not divided. Avoiding spatial discretization deteriorates the precision. If the line is divided into 20 lines of 15 km length each, the waveforms of MoC overlap with the waveforms of ULM as shown in the figures.

Many other line configurations have been tested and a similar pattern is observed, i.e. the results get more precise once the line is subdivided.

Note that the solution with MoC also depends heavily on the time step of simulation. The Fig. 8 shows the receiving end voltages obtained using three different time steps with MoC, 0.1, 1 and 10 μs. The solution closest to the ULM is obtained with 10 μs. Reducing the time step does not necessarily improve the results. However, if the line is subdivided, the results with different time steps start overlapping (not shown). Time step dependence is due to the numerically unstable model. The ULM produces identical results for all the time steps above.

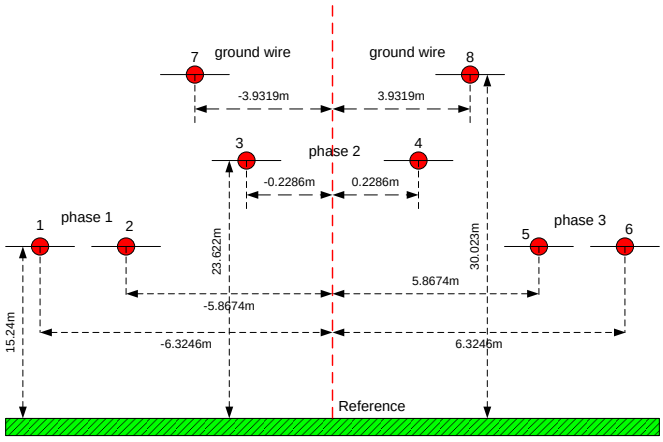

Fig. 3 Transmission Line Case

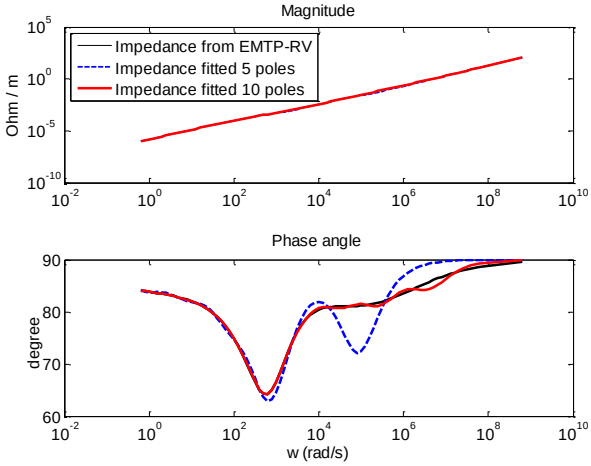

Fig. 4 Fitting for element (2,1) of the series impedance

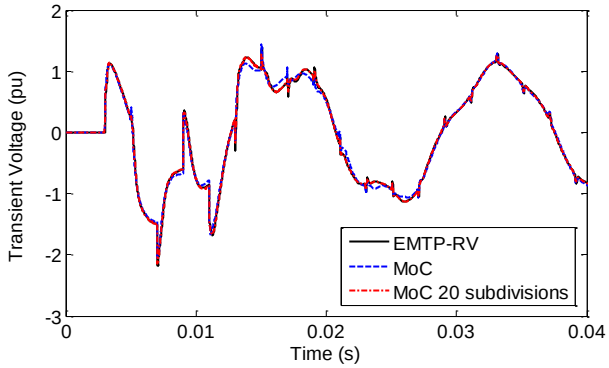

Fig. 5 Voltage of receiving end phase A: Comparison between MoC, MoC with 20 subdivisions and EMTP-RV

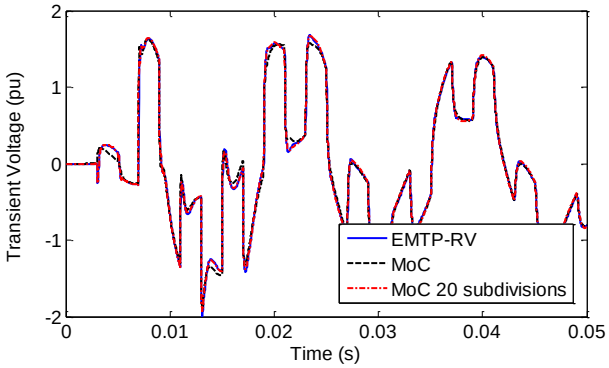

Fig. 6 Voltage of receiving end phase B: Comparison between MoC, MoC with 20 subdivisions and EMTP-RV

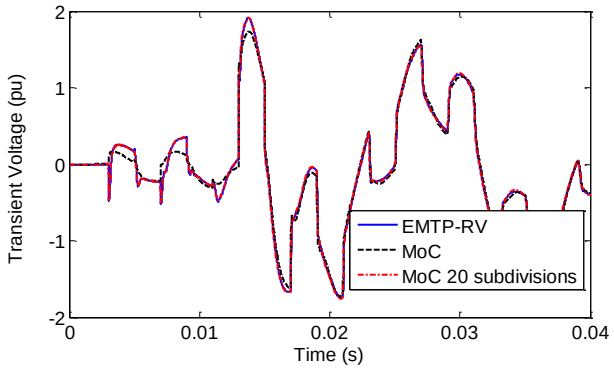

Fig. 7 Voltage of receiving end phase C: Comparison between MoC, MoC with 20 subdivision and EMTP-RV

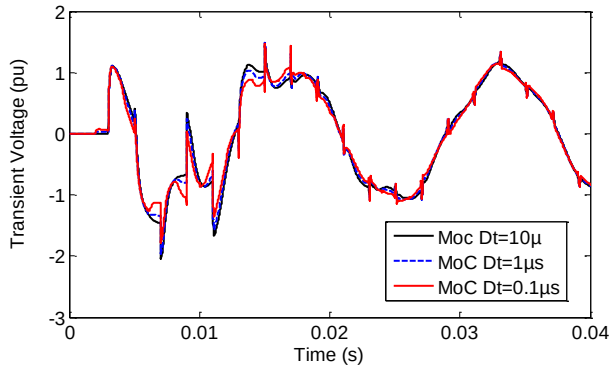

Fig. 8 Voltage of receiving end phase A with the MoC with different time steps

VI. Conclusion

This paper reveals in detail the approximations behind the application of Method of Characteristics for the transient analysis of lines and discusses numerical improvements. The MoC requires spatial discretization in addition to discretization in time as opposed to traveling wave methods. The removal of spatial discretization has been recently discussed in the literature but it results in numerically imprecise line and cable models as shown in this paper. The fundamental source of numerical problems is identified as the approximation error arising from the linearization of differential equations over a large integration step in time. The integration step should be taken as equal to the modal delay corresponding to the fastest mode. Naturally, this error can be minimized by subdividing the line at the expense of increased numerical operations as shown through case studies. On the other hand, the resulting modeling approach can be useful for the visualisation of internal overvoltages or when the transmission line needs to be subdivided due to non-uniform structure or excitation.

References

[1] A. Morched, B. Gustavsen,, M. Tartibi, “A universal model for accurate calculation of electromagnetic transients on overhead lines and underground cables”, *IEEE Trans. on Power Delivery*, vol. 14, No. 3, July 1999, pp. 1032-1038.

[2] H. M. J. De Silva, A. M. Gole, J. E. Nordstrom, L. M. Wedepohl, “Robust Passivity Enforcement Scheme for Time Domain Simulation of Multi-Conductor Transmission Lines and Cables”, *IEEE Trans. on Power Delivery*, vol. 25, no. 2, Apr. 2010, pp. 930-938.

[3] I. Kocar, J. Mahseredjian and G. Olivier: “Improvement of numerically stability for the computation of transients in lines and cables”, IEEE Trans. on Power Delivery, Vol. 25, Issue 2, April 2010, pp. 1104-1111.

[4] B. Gustavsen, "Avoiding Numerical Instabilities in the Universal Line Model by a Two-Segment Interpolation Scheme," *IEEE Transactions on Power Delivery*, vol.28, no.3, July 2013, pp.1643-1651.

[5] A. Semlyen, B. Gustavsen, "Phase-Domain Transmission-Line Modeling With Enforcement of Symmetry Via The Propagated Characteristic Admittance Matrix," *IEEE Transactions on Power Delivery*, vol.27, no.2, pp.626-631, April 2012.

[6] O. Ramos-Leanos, J. L. Naredo, J. Mahseredjian, C. Dufour, J. A. Gutierrez-Robles, I. Kocar, "A Wideband Line/Cable Model for Real-Time Simulations of Power System Transients," *IEEE Transactions on Power Delivery*,, vol.27, no.4, pp. 2211-2218, Oct. 2012.

[7] J.L. Naredo, P. Moreno, A.C. Soudack, J.R. Martí, "Frequency independent representation of transmission lines for transient analysis through the method of characteristics," in *Proc. Athens Power Tech. Nat. Tech. Univ. Athens IEEE/Power Eng. Soc. Joint Int. Power Conf.*, vol. 1, Athens, Greece, Sept. 5-8, 1993, pp. 28-32.

[8] J.L. Naredo, P. Moreno, A.C. Soudack, J.R. Martí, "Frequency independent representation of transmission lines for transient analysis through the method of characteristics," in *Proc. Athens Power Tech. Nat. Tech. Univ. Athens IEEE/Power Eng. Soc. Joint Int. Power Conf.*, vol. 1, Athens, Greece, Sept. 5-8, 1993, pp. 28-32.

[9] A. Ramirez, J.L. Naredo, L. Guardado, "Electromagnetic transients in overhead lines considering frequency dependence and corona effect via the method of characteristics," *Int. J. Electrical Power and Energy Systems*, vol. 23, no. 3, pp. 179-188, Aug. 2001.

[10] A. Ramírez, J.L. Naredo, P. Moreno, "Full frequency-dependent line model for electromagnetic transient simulation including lumped and distributed sources," *IEEE Trans. Power Del.*, vol. 20, no. 1, pp. 292-299, Jan. 2005.’

[11] P. Moreno, A.R. Chavez, J.L. Naredo, "A simplified model for nonuniform multiconductor transmissions lines using the method of characteristics," in *Proc. IEEE/PES General Meeting*, Pittsburgh, 2008, pp. 1-5.

[12] P. Moreno, A. Ambrosio, P. Gómez, "The characteristics approach for modelling single phase transmission lines with frequency dependent electrical parameters," in *IEEE/PES T&D Conference and Exposition*, Bogotá, Colombia, Aug. 2008, pp. 1-4.

[13] .C. Escamilla, P. Moreno, P. Gómez, "New model for overhead lossy multiconductor transmission lines," *IET Generation, Transmission & Distribution*, vol. 7, no. 11, pp. 1185-1193, Nov. 2013.

[14] B. Gustavsen, A. Semley, "Rational approximation of frequency domain responses by vector fitting," *IEEE Tran. Power Del.*, vol. 15, no. 3, pp. 1052-1061, July. 1999.

[15] B. Gustavsen, J. Mahseredjian, "Simulation of Internal Overvoltages on Transmission Lines by an Extended Method of Characteristics Approach," *IEEE Trans. on Power Delivery*, vol. 22, no. 3, July 2007, pp. 1736-1742.

[16] J. Mahseredjian, S. Dennetière, L. Dubé, B. Khodabakhchian and L. Gérin-Lajoie, “On a new approach for the simulation of transients in power systems”, *Electric Power Systems Research*, Vol. 77, Issue 11, September 2007, pp. 1514-1520.